Journal of New Technology and Materials
JNTM
Vol. 01, N°00 (2011)29-32

OEB Univ. Publish. Co.

Photovoltaic applications of Light Beam Induced Current technique

Y. Sayad[(a)], A. Kaminski[(b)], D. Blanc[(c)], B. Bazer-Bachi[(c)] , M. Lemiti[(c)] and A. Nouiri[(d)]
(a) Institut des Sciences et Technologies, Centre Universitaire de Souk Ahras, Souk Ahras, 41000.
(b) IMEP-LAHC, Grenoble INP, Minatec, 3 rue Parvis Louis Néel - BP 257 – 38016 Grenoble Cedex 1, France
(c) Université de Lyon, Institut des Nanotechnologies de Lyon, INL-UMR5270, CNRS, INSA Lyon, 69621 Villeurbanne, France.
(d) Département de Physique, Faculté des Sciences, Université Larbi Ben M'hidi, Oum El-Bouaghi
Corresponding author: Tel. : +213.30.95.29.35 ; email : yassine.sayad@cu-soukahras.dz, say_phy@yahoo.fr
Received: 23 May 2011, accepted: 30 September 2011

Abstract:
Light or Laser beam induced current technique (LBIC) is conventionally used to measure minority charge carrier's diffusion length L_D by scanning a light spot away from collector (abrupt pn junction or Schottky contact). We show here the necessary precautions to be taken in order to apply this method on materials used in photovoltaics. We talk about SRLBIC or spectral response LBIC when this technique is combined with spectral reflectivity to allow determination of cells quantum efficiency. From internal quantum efficiency analysis, one deduces an effective carrier diffusion length, L_{eff}, including bulk and surface recombinations. LBIC is, also, often used to reveal electrically active extended defects such as grain boundaries and dislocations, and to check passivation efficiency of fabricated cells.
***Key words:** LBIC, solar cells, crystalline silicon, diffusion length, extended defects, surface passivation.*

1. Introduction

Since the end of Second World War, the world economy has grown exponentially, which exploded its energy demands. To the head of energy sources coming fossil fuels (oil, gas and coal) which are non-renewable and causing greenhouse gases emissions, which pushed governments in industrialized countries to take decisions to encourage renewable energies sector. To the head of this sector comes photovoltaic industry.

In photovoltaic, crystalline silicon remains the most used material, and the global demand for this material has grown exponentially exceeds, since 2003, integrated circuit industry and the price of solar grade silicon increased from $20\$/kg$to $200\$/kg$ in short period. To face this shortage of silicon, the photovoltaic specialists tend to produce more and more thinner cells (currently cells with less than $180\mu m$theckness are commercialized) and to use less pure materials (compensated metallurgical grade silicon). Emergence of such thin and/or low quality materials has increased needs in characterization techniques.

In this paper, we focus on photovoltaic applications of LBIC technique. We begin with extraction of minority carrier's diffusion length by light spot scanning method in crystalline silicon used in photovoltaic. This method is known since 1980, but its application has not been, always, unmistakable on photovoltaic materials. We, also, see technique capabilities to detect extended defects (grain boundaries and dislocations), and to check passivation efficiency of cells.

2. Extraction of charge carrier's diffusion length in crystalline silicon wafers by light spot scanning method.

The method consists in scanning an laser beam away from collector and recording short circuit current at each point (Fig.1.). A collector structure may be Schottky contact or abrupt pn junction. We have chosen to make Schottky contacts by depositing a very thin (25 nanometers) and transparent Chromium layer, however, a pn junction collect better the photogenerated carriers. We should, also, passivate surface recombination centers before measurements.

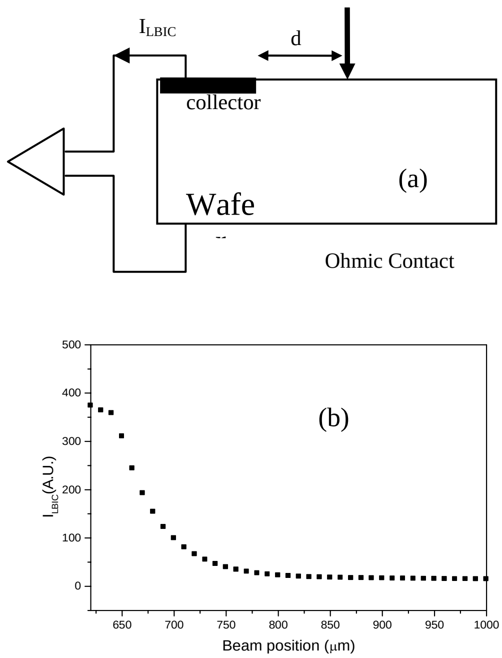

Fig. 1. Measurement structure of induced current (a) and a typical experimental profile obtained using p-Cz sample (b).

Our ISE TCAD simulations [1,2] showed that if silicon wafer hada thickness ofat least four times minority carrier diffus e on length, $\boldsymbol{w > 4L_D}$,
one obtain a photocurrent decay obeying to the following law,

$$I_{LBIC} \propto d^{-n} exp(-d/L_D) \qquad (1)$$

Where n is between 0 and 1.5, L_D is bulk diffusion length.

Table 1 recapitulate measurement results of electrons diffusion length in a thick p type multicrystalline silicon sample (2.5mm) with resistivity of $0.5\,\Omega.cm$. The frontal surface is passivated by a hydrogen rich double dielectric layer SiOx/SiNy. Carrier collector is a Schottky contact formed by deposition of thin chromium layer, and measurements were performed in different grains.

Table. 1. Diffusion length in a thick p type silicon

n	L_D (µm)
0.34	58
1.33	70
0.43	190
1.02	419
0.59	395
1.03	520

In relatively thin wafers, where $w < 4L_D$, which is always the case of mono and multi crystalline silicon wafers used for fabrication of solar cells, where $L_D \sim w$, one obtain a simple exponential decay,

$$I_{LBIC} \propto exp(-d/L_{eff}) \qquad (2)$$

Where, L_{eff} , is an effective diffusion length including bulk and surface recombination. Our simulations [1,2] shows that L_{eff} value becames very close to L_D for low recombination velocities of carriers at surfaces (fig. 2). Practically, one can reach carriers recombination velocities around $20\,cm.s^{-1}$ using silicon thermal oxide, SiO_2.

Figure 3 shows a photocurrent profile in semi-logarithmic scale, obtained on thin layer of p-type crystalline silicon (50 microns). This thin layer was epitaxially grown on a thick and highly doped CZ substrate, P+. The frontal surface was passivated in Hydrogenated silicon nitride SiNx:H. The collector is a Schottky contact obtained by deposition of thin Chromium layer.

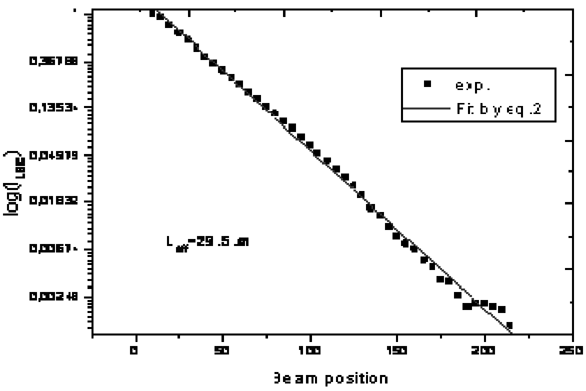

Fig.2. Extraction of diffusion length

3. **Extraction of charge carriers diffusion length in finished cells.**

In fabricated cells, one can deduce carrier's diffusion length from spectral analysis of cell internal quantum efficiency. In this case, one measure short circuit current $(I_{SC})$and reflectivity (R)at each wavelength, then, one deduce internal quantum efficiency using following relationship,

$$IQE(\lambda) = \frac{hc}{\lambda q P_{in}(\lambda)} \frac{I_{SC}(\lambda)}{(1-R(\lambda))} \qquad (3)$$

$P_{in}(\lambda)$ is incident beam power at wavelength λ .

In other hand, Basore [3] showed that in spectral domain$[800nm, 1000nm]$, the inverse the quantum efficiency is related to light absorption depth by following relationship,

$$IQE^{-1} = 1 + \frac{1}{L_{eff}}\left(\frac{1}{\alpha}\right) \qquad (4a)$$

Where L_{eff} is an effective diffusion depends on bulk diffusion length L_D and electrons recombination velocity at cell rear surface, S_r.

$$L_{eff} = L_D \left[\frac{\frac{S_r L_D}{D} + tanh\left(\frac{W}{L_D}\right)}{1 + \frac{S_r L_D}{D} tanh\left(\frac{W}{L_D}\right)}\right] \qquad (4b)$$

We note that effective diffusion length approaches the bulk diffusion length, $L_{eff} \sim L_D$, for $\frac{W}{L_D} > 1$.

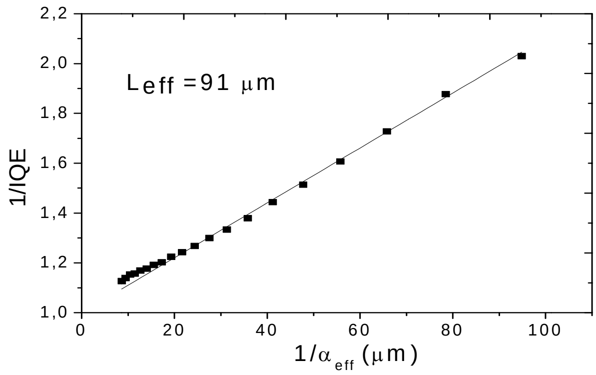

Fig. 3. Internal quantum efficiency inverse versus light penetration depth of commercial solar cell, effective diffusion length of $91\mu m$ is obtained by fitting to eq.3.

4. **Highlighting extended defects in solar cells.**

Extended defects such as grain boundaries and dislocations are preferential sites for segregation of impurities and points defects, and causes photocurrent loss in solar cells.

Figure 4 shows cartography of square areas $(1.5cm \times 1.5cm)$ of commercialized solar cell performed by 532nm laser diode (which corresponding to depth absorption of light of $1.3\mu m$) with scanning step of $50\mu m$. This cartography shows bright and dark grains, which corresponding a high and low carrier lifetime grains, respectively.

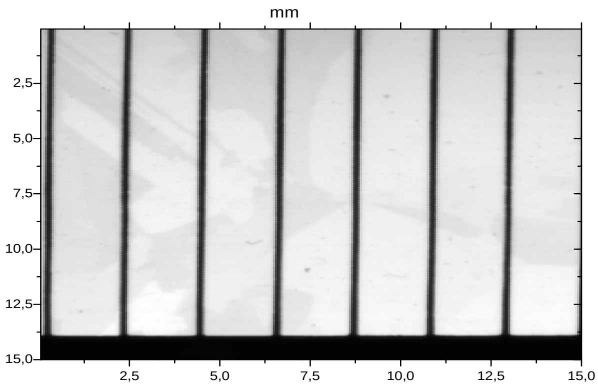

Fig. 4. LBIC cartography of a square surface $(1.5cm \times 1.5cm)$ performed by à 532nm laser $\left(\frac{1}{\alpha} = 1.3\mu m\right)$, with a scanning step of $50\mu m$.

LBIC profiles, like the showed one in figure 5, may be analyzed using analytical models [4-7] to extract minority carrier recombination velocity at grain boundary.

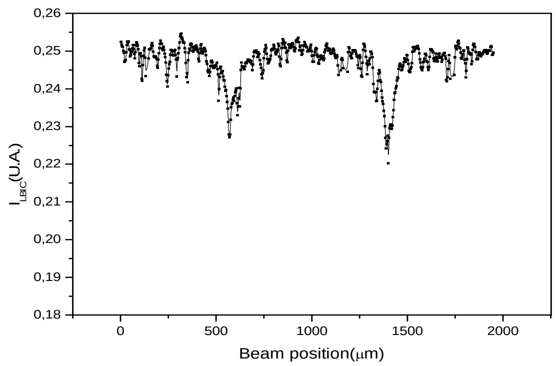

Fig.5. LBIC signal measured with 632nm laser in vicinity of two adjacent grain boundaries in silicon solar cell. Beam spot size at cell surface is about $6\mu m$.

31

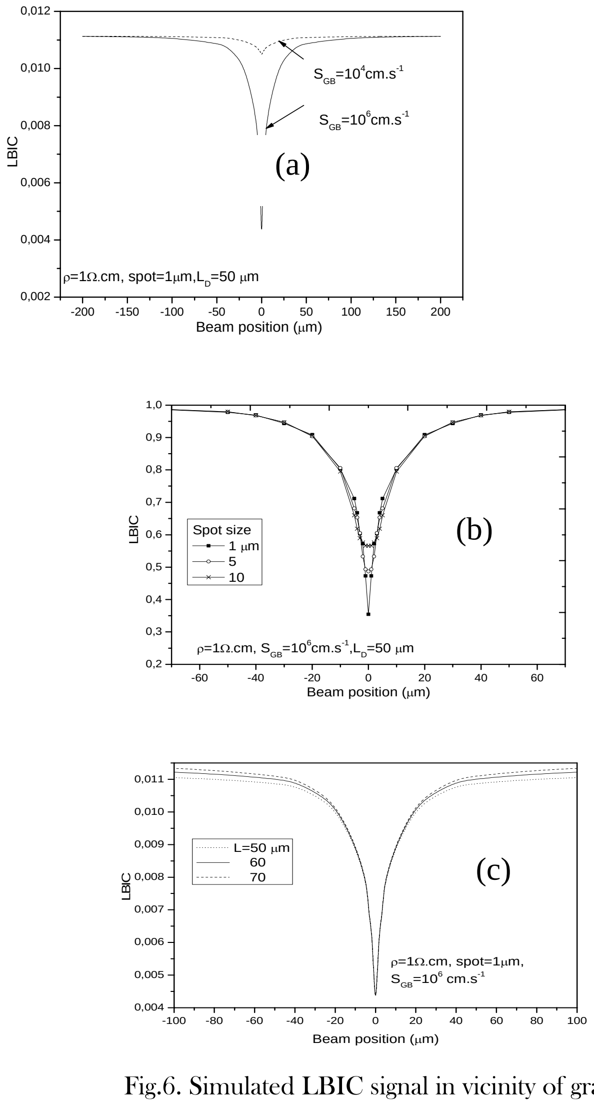

Fig.6. Simulated LBIC signal in vicinity of grain boundary. Impact of carrier recombination velocity (a), spot size (b) and diffusion length (c)

Figure 6 show ISE TCAD simulations of photocurrent at vicinity of grain boundary under different conditions of recombination velocity at grain boundary (a), spot size (b) and of carrier diffusion length (c).Dislocations may be origin of shorts in solar cells and, thus, decreases cell shunt resistance. Figure 7 shows cartography of a square area ($1cm \times 1cm$) of one solar cell, this cell have previously undergone a thermal annealing at 850°C of one hour duration before emitter diffusion step. The cartography shows formation of dislocations in high density.

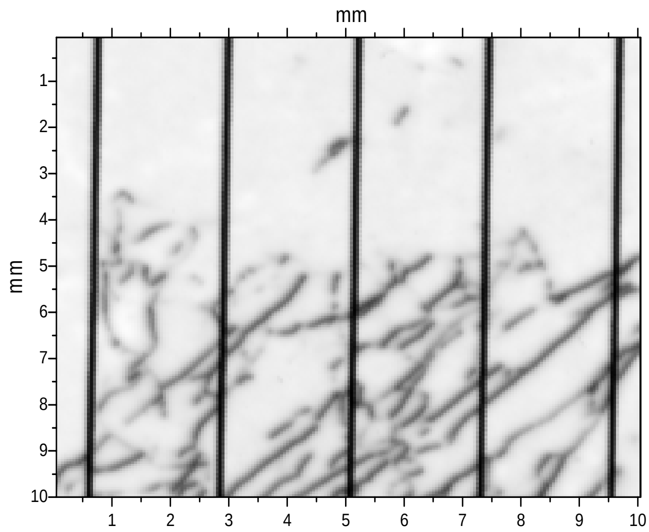

Fig. 7. LBIC cartography of square surface $(1cm \times 1cm)$ performed by 980nm laser $\left(\frac{1}{\alpha} = 103\mu m\right)$, with step of $50\mu m$. Spot size at cell surface is $11\mu m$.

5. Displaying passivation efficiency.

Cartography of photocurrent may be used to compare passivation efficiency at different cell places. In figure 8, LBIC cartography of a solar cell measured by 980nm laser diode, the cell rear surface is passivated by triple dielectric layers (SiNx and SiOx). We remark a more photocurrent in areas passivated by dielectric layers than at localized grid of BSF (back surface field).

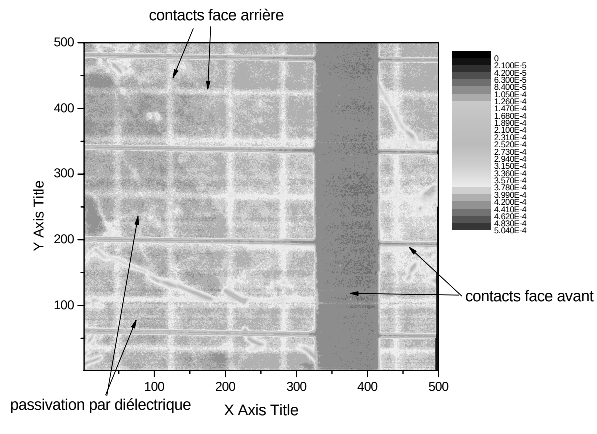

Fig.8. LBIC cartography of solar cell using 980nm laser diode, the cell rear surface is passivated by triple dielectric layers. Scanning step is 20 μm.

6. Conclusion

Using LBIC technique one can determine charge carriers diffusion length in silicon thin films and wafers, as well as in finished cells. This allows assessing possible degradation or improvement of starting material quality during cell process.

LBIC cartographies using different wavelengths allow probing cells from frontal to rear surfaces, to view electrically active defects and to evaluate passivation efficiency.

References :

[1] Y. Sayad, A. Kaminski, D. Blanc, A. Nouiri and M. Lemiti, Superlattices and Microstructures 45 (2009) 393-401

[2] PhD Thesis (online): *Détermination de la longueur de diffusion des porteurs minoritaires dans le silicium cristallin par interaction lumière-matière.*2009, INSA de Lyon.

[3] P.A. Basore, 23rd IEEE Photovoltaic Specialists Conference, 1993, p. 147-152.

[4] J. Marek, J. Appl. Phys., vol.55, Issue 2,1984, pp.318-326.

[5] J. D. Zook, Appl. Phys. Lett., vol. 42, Issue 7, 1983, pp.602-604.

[6] C. Donolato, J. Appl. Phys., vol. 54, Issue 3, 1983, pp.1314-1322.

[7] A. Mittiga and M. Capizzi, J. Appl. Phys., vol. 62, Issue 18, 1987, pp. 3443-3445.